

## MEASUREMENT OF RF ACCELERATOR CAVITY FIELD LEVELS AT HIGH POWER FROM X-RAY EMISSIONS\*

G. O. Bolme, G. P. Boicourt, K. F. Johnson, R. A. Lohsen, O. R. Sander, and L. S. Walling  
 Los Alamos National Laboratory, Los Alamos, NM 87545

### Abstract

Energy spectroscopy measurements of x-rays from rf structures at high power provide an independent method of finding accelerating-gap voltages in the multiple-cell accelerating structures. An x-ray detector is used to measure the energy of the emitted x-rays; and the high-energy endpoint of the energy spectrum histogram corresponds with the peak-gap voltage in the rf structure. The x-ray measurements are used to provide a calibration relating peak-gap voltage to rf structure field sampling probes. The analyzed x-ray data has been compared to theoretical SUPERFISH and MAFFIA3D predictions and to beam-dynamics data for the multiple-cell structures. Information about this diagnostic technique and its value for verifying accelerator modeling codes is presented.

### Introduction

A primary objective of the GTA program is verification of the accelerator modeling codes. Codes such as the SUPERFISH family of codes and MAFFIA3D model the performance of the rf structures; and particle-dynamics codes such as PARMTEQ and PARMILA predict beam parameters based on rf structure simulations. RF power and measured Q have been used to predict the field levels by means of the rf structure modeling codes; and these predicted field levels are applied as an input to the particle dynamics codes to generate the expected beam characteristics. Thus, experimental verification of code performance has bridged both sets of codes by correlating measured beam parameters to the rf structure power consumption. Our rf cavity gap-voltage measurements using the x-ray emissions, determine the accelerating structure electric field levels—the interconnecting parameter of these two sets of accelerator modeling codes.

A direct measurement of the rf structure fields cannot be accomplished because any probe capable of measuring the full-field level would significantly perturb the cavity. A measurement of the rf structure x-ray emissions is nonintrusive on the cavity and its operation; therefore, an x-ray diagnostic system does not perturb or modify the rf structure. Our diagnostic apparatus is based on an x-ray spectroscopy system, which measures the energies of individual x-rays outside the accelerator cavity vacuum vessel. The upper end-point energy of the x-ray energy spectrum corresponds to the peak-gap voltage from which the electric field levels can be extrapolated. Sets of these data

provide the scaling relation between cavity power and field level, and this scaling relation provides the field level correlation for beam data relating cavity power to beam parameters.

### RF Structure X-ray Emissions

High-voltage gaps in a vacuum environment are well-known sources of x-rays. The rf accelerator sections are fabricated assemblies of one or more resonant electromagnetic cells, creating high-voltage gaps that the beam particles transit. These oscillating, high-voltage gaps are necessarily contained within a high-vacuum vessel; therefore, the accelerator sections are prolific sources of x-ray emissions under normal operation.

The source of these x-rays is a multistep process depicted in Fig. 1. The high voltage across any gap is associated with electric fields throughout the physical region of the gap. At the negatively-charged surface of the gap, the electric fields result in the field emission of electrons into the

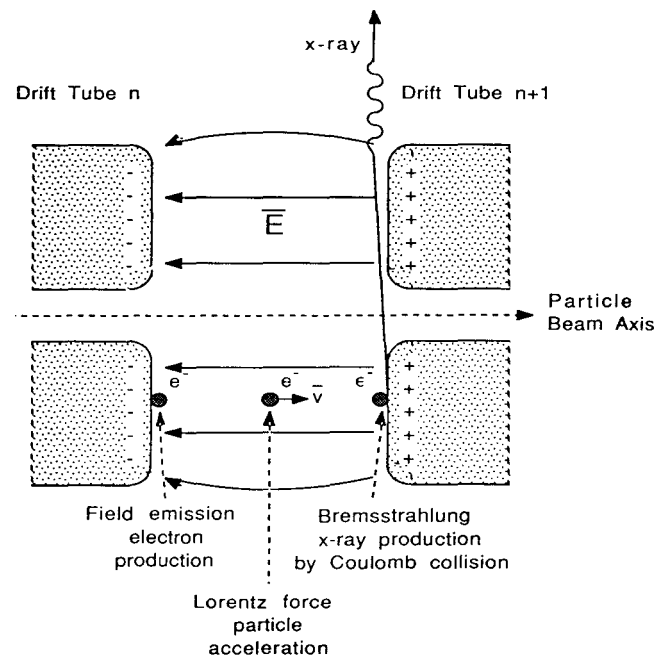


Fig. 1. Source of the rf structure x-ray emissions at high-power.

\*Work supported and funded by the Department of Defense, US Army Strategic Defense Command, under the auspices of the Department of Energy.

vacuum gap. These electrons are accelerated within the gap by the fields present; and in transiting the gap, each electron attains a kinetic energy associated with almost all of the gap voltage,  $V_g$ .<sup>1</sup>

$$\begin{aligned} T &\equiv \text{Electron kinetic energy} \\ &\approx eV_g \end{aligned} \quad (1)$$

At the positively-charged surface, these accelerated electrons lose their energy in Coulomb collisions, thus, emitting Bremsstrahlung x-rays. The x-rays have a full distribution of energies up to the full kinetic energy of the accelerated electrons. The angular distribution of these x-rays is strongly peaked in the forward direction of the incident electron; however, a finite number of x-rays are emitted throughout the full solid angle.<sup>2</sup> It is these emitted x-rays that carry the signature of the gap voltage, and their penetration outside the vacuum confinement wall provides us with an indirect means of measuring the gap voltage without perturbing the cavity structure or the fields within.

### Apparatus

The x-ray detection system is based on a Canberra HPGe detector with a measured FWHM resolution  $\leq 1\%$  across the energies of interest. The detector analog signal is shaped by a spectroscopy amplifier and converted to digital data by a voltage-sensitive ADC. In order to reduce background and to limit x-ray data collection to the rf pulse, logic electronics are used to gate ADC conversion for x-rays occurring only during the rf pulse. All analog and logic signal processing, as well as digital conversions, are done by NIM electronic modules.

The data collection, display, and storage have been done by two different computer systems—a DEC microVAX and an IBM-PC. For both computer systems, the interface to the ADCs is controlled through CAMAC hardware.

Because many of the rf structures are multiple-cell rf cavities, it is necessary to limit the detector view to one cell of the accelerator structure. It is desirable to have an unobstructed view of the acceleration cell (voltage gap) of interest through a glass vacuum window. The glass vacuum window aids in the alignment of the x-ray detector, assists in verifying that the detector view is restricted to a single cell, and allows  $\approx 100\%$  transmission of x-rays above 20 keV. The HPGe detector is placed in a lead shield from 0.5-in. to 2-in. thick (measurement dependent) in order to block detection of x-rays from other structure cells, the rf amplifiers, or surrounding material that can scatter x-rays. The detector and lead shield are positioned as far back from the accelerating structure as geometry permits in order to further reduce count rate and background rate. Lead collimators with apertures of 0.040 in. to 0.250 in. are used to restrict the detector view to a single voltage gap and to control the x-ray counting rate. Tin, copper, aluminum, and lead sheets are placed over the collimator aperture to further control the x-ray counting rate as required. The planview of the detector apparatus is shown in Fig. 2.

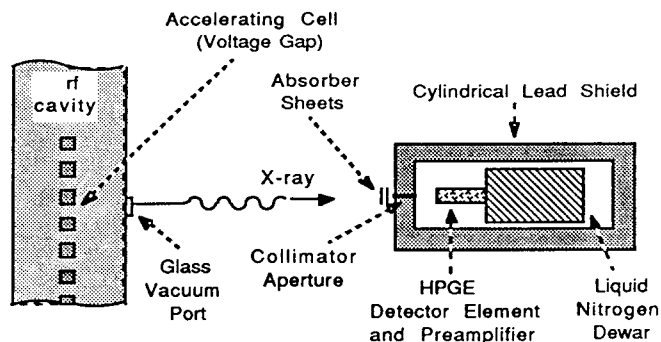


Fig. 2 Experimental planview for the x-ray emission apparatus.

### Measurement Procedures

After configuring the apparatus according to Fig. 2, a  $^{133}\text{Ba}$  x-ray source is positioned in front of the detector element for energy calibration of the detector system. The calibration data are collected without the rf timing gate until statistics are sufficient for good resolution of the x-ray lines. Occasionally, a second calibration data set is taken with the required rf timing gate and operating rf amplifiers to ensure that rf noise pick-up is not affecting the x-ray signals. The calibration is not normally taken in this mode due to the excessive time required for good statistics at the low rf duty factor.

The rf power is turned on to the desired level and the rf timing logic gate is set to window the center of the rf pulse. By restricting x-ray data collection to a time window at the center of the rf pulse, excess background and x-ray data associated with the transients of rf turn-on and turn-off are eliminated. The absorber foils and collimator aperture are then adjusted to limit the counting rate to 0.25 to 1.0 x-ray for each 500  $\mu\text{sec}$  of rf pulse duration. Limiting the x-ray counting rate in this manner significantly reduces the pulse pile-up at the high-energy end of the data spectrum.

With the data rate adjusted, an x-ray data spectrum is collected at the fixed rf level until sufficient statistics are collected to permit fitting to the energy endpoint. An additional x-ray spectrum is taken with the collimator aperture blocked and the remaining configuration identical to data collection. This spectrum represents the background within the data spectrum. If the background counting rate is insignificant, a very short measurement is made; however, if the background rate is sizable, a longer measurement is made to permit a time-weighted subtraction of the background from the x-ray data prior to doing the energy endpoint fit.

### Data Analysis

The x-ray data from the ADC is stored in the form of a histogram of counts versus ADC channel number. The

$^{133}\text{Ba}$  x-ray source is used to energy scale the ADC channel number, because it has several, well-resolved x-ray lines and the two dominant x-ray lines (81.0 keV and 356.0 keV) bracket the energy endpoints of most of the rf structures. A least-squares fit with a Gaussian peak is made of the two dominant x-ray lines in the spectrum using the code, CURFIT.<sup>3</sup> A straight-line scale of x-ray energy versus ADC channel number is calculated from the peak centers of the 81.0 keV and the 356.0 keV x-ray lines.

With an energy calibration for the x-ray spectrum, the rf structure data can be fitted for the energy endpoint. If significant background radiation was detected, a time-weighted background spectrum is subtracted from the x-ray spectrum. A straight-line, least-squares fit is made of the x-ray spectrum with the code, CURFIT,<sup>3</sup> in order to project the largest possible x-ray energy. Since pulse pile-up creates a turn up at the high-energy end of the spectrum, a fitting window is set across a linear region of the energetic x-rays to most accurately project the spectrum endpoint. A sample of an rf structure x-ray spectrum and endpoint fit are displayed in Fig. 3.

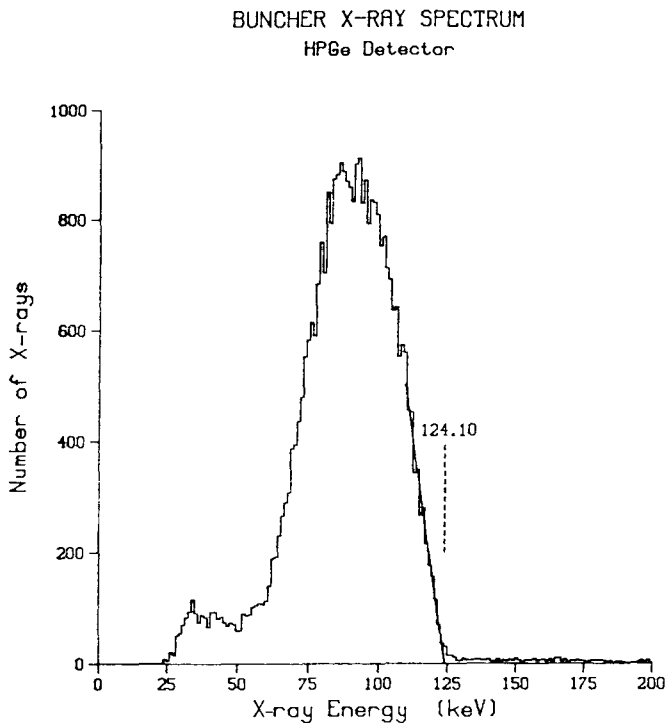


Fig. 3. Rf structures x-ray emission data spectrum.

A single x-ray energy endpoint does not provide an accurate prediction of peak-gap voltage as a function of rf power. For this reason, it is desirable to determine the energy endpoints for a minimum of 5 rf power levels. With multiple energy endpoints, a least-squares fit is made of

endpoints versus power using the known  $\sqrt{x}$  dependence. The fit is again made using the code, CURFIT.<sup>3</sup> The  $\sqrt{x}$  dependence scale of this fit is now useful in correlating to the accelerator beam data. An example of a voltage-power fit is shown in Fig. 4.

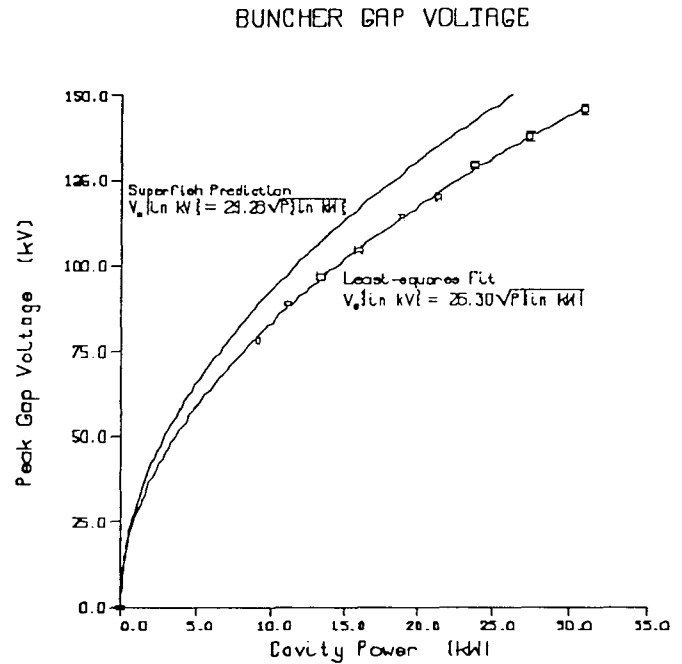


Fig. 4. Gap voltage versus rf structure power.

### Discussions

Because the correlation between beam parameters and field level for the multiple-cell structures is primarily in beam quality and largely independent of the beam energy, the field amplitude measurement accuracy cannot be determined from the beam parameters of the multiple-cell structures. The best-accuracy estimate of the ATS diagnostic system is made from the beam energy gain/loss measurements of single- and double-cell structures. For single- and double-cell structures, the correlation of the energy measurements to the gap voltage is dependent only on the transit time factor for the beam in the structure and the accuracy of the energy measurements. The Cryo-DTL sparker and the four rebuncher cavities of the ATS funnel experiment have given us five independent beam energy correlations for the gap-voltage measurements. The comparisons for these structures are given in Table 1. The absolute beam energy error of the LINDA<sup>4</sup> data is 4 to 5 keV and the beam energy error of Phase-Scan<sup>5,6</sup> is unknown. The large discrepancy for the R3 and R4 data is unknown but is likely due to poor geometry between the voltage gap and the x-ray detector. Based on this information and the previous discussions, we have assigned an estimated accuracy of  $\pm 5\%$  to the accuracy of the x-ray emission diagnostic system.

**TABLE 1**  
**Beam Energy Gain/loss Measurement for Single and Double Cell rf Structures**

| Cavity | X-Ray Prediction (keV) | Measured (keV) | Difference % | Diagnostic |
|--------|------------------------|----------------|--------------|------------|
| CDTL   | 535                    | 565            | -6           | Phase-Scan |
| R1     | 197.9                  | 197            | <1           | LINDA      |
| R2     | 157.1                  | 151            | +4           | LINDA      |
| R3     | 76.2                   | 88             | -15          | LINDA      |
| R4     | 142.3                  | 161            | -13          | LINDA      |

### Conclusions

The x-ray measurement of peak-gap voltages and field levels has been applied to all of the structures used in the ATS program, all ATS support sparker experiments, the rf Seal Test Cavity, and the BEAR RFQ. For every structure, it has benchmarked the cavity field levels relative to rf power levels.

The field levels measured by the characteristic x-ray emissions have also provided an important reference for much of the ATS beam data. These measured field levels have provided a check on rf structure stability, verified that sufficient fields were achieved during conditioning for operation, and provided a measured field value for comparison of beam parameters to code predictions. As it exists, this diagnostic has reached the maturity to provide useful information for accelerator operations on GTA.

### References

1. R. Hawley, "Electron Emission from Metallic Surfaces," High-Voltage Technology, Oxford University Press, London (1968), pp 95-110.
2. J. D. Jackson, Classical Electrodynamics, John Wiley and Sons, Inc., New York (1975), pp 701-15.
3. P. R. Bevington, Data Reduction and Error Analysis for the Physical Sciences, McGraw-Hill, Inc., New York (1969), pp 237-9.
4. W. B. Cottingham, G. P. Boicourt, J. H. Cortez, W. W. Higgins, O. R. Sander, and D. P. Sandoval, "Noninterceptive Technique for the Measurement of Longitudinal Parameters of Intense H<sup>-</sup> Beams," Proc. 1985 Particle Accelerator Conference, *IEEE Trans. Nucl. Sci.* **32** (5), (1985) 1871.
5. J. D. Gilpatrick, R. E. Meyer, F. D. Wells, J. F. Power, and R. E. Shafer, "Synchronous Phase and Energy Measurement System for a 6.7 MeV H<sup>-</sup> Beam," 1988 Linear Accelerator Conference, Williamsburg, Virginia, October 1988, Continuous Electron Beam Accelerator Facility CEBAF-Report-89-001 (June 1989), 134.

6. J. D. Gilpatrick, L. Burczyk, C. Fite, B. Gunther, R. Meyer, J. Power, R. B. Shurter, and F. D. Wells, "Overview of the Microstrip Beam Diagnostics," 1989 Neutral Particle Beam Technology Symposium, Monterey, CA, July 1989.